Pak. J. Bot., 57(2): 469-479, 2025. DOI: http://dx.doi.org/10.30848/PJB2025-2(37)

SYNTHESIS AND CHARACTERIZATION OF CALCIUM OXIDE NANOPARTICLES AND EVALUATING THEIR DIVERSE EFFECTS ON PLANT GROWTH AND DEVELOPMENT OF *TRIGONELLA FOENUM GRAECUM* L.

HARISH KRISHNAN[1], MANOJ KUMAR SRINIVASAN[1], BICHANDARKOIL JAYARAM PRATIMA[1], BRISKA JIFRINA PREMNATH[1], KAMALESH BALAKUMAR VENKATESAN[1], NALINI NAMASIVAYAM[1*], CHELLASAMY PANNEERSELVAM[2,3*], MOHAMMED ALI ALSHEHRI[2], SAMY SAYED[4] AND SATHISH-KUMAR KAMARAJ[5]

[1]Department of Biochemistry and Biotechnology, Faculty of Science, Annamalai University
[2]Department of Biology, Faculty of Science, University of Tabuk, Tabuk 71491, Saudi Arabia
[3]Biodiversity Genomics Unit, Faculty of Science, University of Tabuk, Tabuk 71491, Saudi Arabia
[4] Department of Economic Entomology and Pesticides, Faculty of Agriculture, Cairo University, Giza 12613, Egypt
[5] Instituto Politécnico Nacional (IPN)-Centro de Investigación en Ciencia Aplicada y Tecnología Avanzada, Unidad Altamira (CICATA-Altamira), Carretera Tampico-Puerto Industrial Altamira Km 14.5, C. Manzano, Industrial Altamira, 89600 Altamira, Tamps., Mexico
** Corresponding author's bionalini@gmail.com and cpselva@ymail.com*

Abstract

The current study aims to investigate the effects of calcium oxide nanoparticles (CaO NPs) on fenugreek (*Trigonella foenum-graecum* L.) and its effect on plant growth and development. The CaO NPs were synthesized by co-precipitation method, and their physicochemical properties were characterized by UV–visible spectroscopy, X-ray diffraction (XRD), Fourier transform infrared spectroscopy (FTIR), Scanning electron microscopy (SEM) and Energy dispersive X-ray spectroscopy (EDS). The XRD result demonstrates that the CaO NPs produced had a hexagonal structure with an average crystallite size of 24 nm and nanoparticle aggregations. CaO NPs were successfully synthesized, as evidenced by the appearance of distinct peaks in the UV-Visible spectroscopy, FTIR, and EDS spectra. The seedlings were tested in greenhouse trials for 16 days at two different concentrations (50 mg. L^{-1} and 100 mg. L^{-1}) to measure the effect of CaO NPs on the growth and development of *Trigonella foenum-graecum L.* The low concentration (50 mg. L^{-1}) of CaO NPs effectively improved the growth parameters (root and stem length, increased leaf area) and some biochemical aspects such as photosynthetic pigments (chlorophyll a, chlorophyll b, carotenoids, and anthocyanins content) and non-enzymatic antioxidants (phenolic content) as well as enzymatic antioxidant enzymes (SOD and CAT) of the plants. Further, MDA concentration was decreased in the treatment with 50 mg. L^{-1}. The growth stagnated or had no impact or slight effect at high concentrations (100 mg. L^{-1}) on *Trigonella foenum graecum* L. plants. Finally, we can conclude the growth-friendly effects of CaO NPs at lower concentrations (50 mg. L^{-1}) on *Trigonella foenum-graecum* L.

Key words: *Trigonella foenum-graecum* L., Fenugreek, Antioxidant, Lipid peroxidation, Calcium oxide nanoparticles.

Introduction

The fabrication of nanomaterials has attracted increasing attention in recent years. They have a size range of 1 to 100 nm. A recent technological advancement is nanoparticles which are widely used in various fields, including skin care products, cosmetics, particularly toothpaste, sunblock, decomposition of organic wastewater treatment, and air cleaning products. Due to their high surface area, and optical and magnetic properties, nanoparticles have recently attracted significant attention. Since most biological molecules have comparable sizes to nanoparticles, many scientists exploited them for *In vivo* and *In vitro* biomedical research and applications. Nanomedicine NPs have potential use in drug delivery (Kumari *et al*., 2023), cancer therapy (Srinivasan *et al*., 2024), bacteria-targeting as an alternative to antibiotics, and antibacterial vaccinations to prevent bacterial infections (Venkatesan *et al*., 2023; and Jadhav *et al*., 2022). Nanoparticles are excellent at sensing and detecting biological structures and systems. Nanoparticles exhibit a variety of agricultural biotechnology applications. Nanoparticles have distinctive physicochemical characteristics and the capacity to increase plant metabolism. For plants to grow and develop, different fertilizers must be used. The majority of fertilizers, however, are ineffective due to a variety of reasons, including leaching, hydrolysis, photolysis degradation, and decomposition. The nanoparticles must explore new applications for nanotechnology and nanomaterials to maximize agricultural output and reduce nutrient losses during fertilization. They may release nutrients on demand, manage the release of chemical fertilizers, and enhance target action (El Briak *et al*., 2002; Habte *et al*., 2019).

Applying nanoparticles to agriculture is an issue right now since it encourages crop growth and productivity while reducing the usage of chemical fertilizers (Tang *et al*., 2008). Nanoparticles may have a big impact on plants when they are introduced. As a result, they may be used in agricultural applications to boost crop production and growth (Amin Alavi & Morsali, 2010).

The current study involves the fabrication of calcium oxide nanoparticles (CaO NPs) by the co-precipitation method, their characterization using various techniques, and their effect on the *Trigonella foenum-graecum* L., plant growth and development. Besides our study was designed to determine whether CaO NPs were suitable for agriculture and to minimize environmental concerns before these composts were recycled back to agricultural land. To assess the impact on the growth and development of CaO NPs, *Trigonella foenum graecum* L., was used as a model. When temperatures are normal, calcium oxide is a crystalline solid and is a white, caustic, alkaline substance, animals and humans can safely use CaO NPs.

Fenugreek (*Trigonella foenum-graecum* L.) is an herb, popular in Egypt including other Middle Eastern nations and Indian subcontinent. *Trigonella foenum-graecum* L., is a useful plant with leaves and seeds commonly used as a spice in culinary preparations and as a component in traditional medicine because of its good taste and fragrance (Bharathiraja *et al*., 2018). It has a lot of vitamins and minerals, such as calcium, iron, nicotinic acid, choline, alpha-carotene, and vitamins A, B1, B2, and C. Besides the presence of lysine- and L-tryptophan-rich proteins, mucilaginous fibre, and other uncommon chemical elements such as coumarin, sapogenins, saponins, phytic acid, and trigonelline are believed to be therapeutically effective. *Trigonella foenum-graecum* L., may prevent cholesterol absorption, which might reduce blood sugar levels (Syed *et al*., 2020). Additionally, *Trigonella foenum-graecum* L., seed extract (methanol, dichloromethane, ethanol, acetone, hexane, and ethyl acetate) contains phenolic acids and flavonoids, which have antioxidant properties (Visuvanathan *et al.,* 2022).

To investigate the defence and tolerance impacts of CaO NP, we analyzed the *Trigonella foenum-graecum* L. seedlings growth responses, photosynthetic activities, antioxidant enzyme activities as well as non-enzymatic antioxidant activities, and lipid peroxidation after 16 days of treatment with 50 mg. L^{-1} and 100 mg. L^{-1} of CaO NPs.

Material and Methods

Chemicals: Calcium chloride dihydrate, sodium hydroxide, sodium hypochlorite, Hoaglands nutritional solution, quercetin, gallic acid, bovine serum albumin (BSA) were purchased from HiMedia Laboratories Private Limited. Bradford protein assay kit was purchased from BioRad.

CaO NPs synthesis and characterization: The calcium chloride dihydrate was dissolved in deionized water and continuously stirred. Stirring continued even after the calcium chloride precursor was fully dissolved. After that, 1 M sodium hydroxide was slowly added to the calcium chloride-containing aqueous solution heated to 80°C and violently agitated. Calcium hydroxide ($Ca(OH)_2$) precipitated out as a white material as sodium hydroxide was added. The addition of sodium hydroxide was ultimately stopped at pH 11.2. The mixture was then precipitated, filtered, and washed with distilled water to eliminate any leftover unreacted substances. This product was dried at 100°C overnight before being thoroughly pulverized with an agate mortar. The resulting $Ca(OH)_2$ fine powder was calcinated in a muffle furnace for 3 h at 600°C. The $Ca(OH)_2$ was decomposed into CaO during calcination. Figure 1 represents the synthesis of CaO NPs. The synthesized nanoparticles were characterized using UV–visible spectroscopy, X-ray diffraction (XRD), Fourier transform infrared spectroscopy (FTIR), scanning electron microscopy (SEM), and energy-dispersive X-ray spectroscopy (EDX).

Plant components and growth conditions: Seeds of *Trigonella foenum-graecum* L., were obtained from the Department of Agriculture, Annamalai University, Chidambaram, Tamil Nadu. Seeds were cleaned for 10 min with 2% sodium hypochlorite, well mixed to eliminate the disinfectant, and then immersed in distilled H_2O at 4°C for 24 h (Reid, 1971). 20 seeds in 9 cm petri plates were incubated for three days at 24-26°C in the dark with two sheets of filter paper and 10 mL of distilled H_2O. *Trigonella foenum-graecum* L., plants were transplanted into pots in Hoaglands nutritional solution (Gamborg and Wetter, 1975), which contained two concentrations (50 and 100 mg. L^{-1}) of CaO NPs or did not (control). CaO NPs preparations were ultrasonically treated for 60 min and kept in the dark. Growth required a 16:8 light-to-dark cycle, 25°C, and 70% relative humidity. Four days once nutrient solutions were changed. A greenhouse test was done with five replicas and forty seeds in each pot.

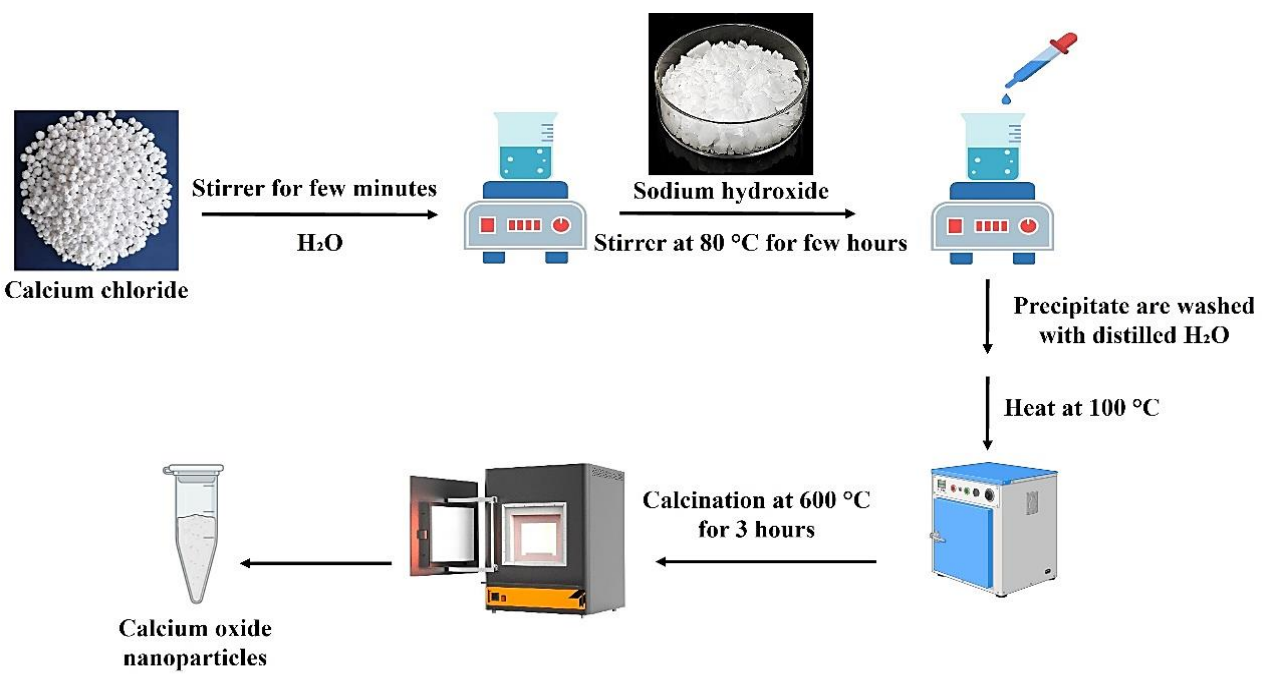

Fig. 1. Synthesis of CaO NPs.

Determination of the seedling growth: The CaO NPs treated and control seedlings were properly cleansed with deionized water every four days for up to 16 days to eliminate nanoparticles and nutrients from the surface. The seedlings' growth rates were then assessed.

Measurement of the stem length, root length, leaves area and water content: Measured the stem, root and leaves from the base to the top using a ruler. Recorded the value in centimeters. For water content, weighed the fresh stem and leaves (initial weight), then dried it in an oven at 60°C until a constant weight was achieved. Weighed the dried sample (dry weight) to calculate water content using the following formula:

$$\text{Water content (\%)} = \frac{\text{Initial weight - Dry weight}}{\text{Initial weight}} \times 100$$

Measurement of photosynthetic pigments: In a mortar and pestle, 100 mg of leaf from seedlings in control and fresh leaves 100 mg from treatment groups were taken. Next, 5 mL of ice-cold acetone (80% (v/v)) was added to separate groups and dissolved. The carotenoids in the pigment extract were measured at 470 nm and chlorophyll at 647 and 663 nm and compared with a blank containing 80% (V/V) acetone. Using Cakmak & Marschner (1992), formulas, the quantities of carotenoid pigments and chl A and B were measured, which is reported as mg/g FW.

Chl A ($\mu g\text{-}mL^{-1}$) = 12.21 A_{663}–2.81 A_{646}
Chl B ($\mu g\text{-}mL^{-1}$) = 20.13 A_{646}- 5.03 A_{663}
Car ($\mu g\text{-}mL^{-1}$) = (1000 A_{470}–3.27 Chl A–104 Chl B)/229

Determining the amount of anthocyanins: According to Gould *et al*., (2000) method, the tissue was frozen and pulverized using a glass pestle. Frozen tissues were quickly submerged in acidified methanol (methanol: H_2O: HCl-16:3:1). The amount of anthocyanin was determined spectrophotometrically at wavelengths of 530 nm and 653 nm. The quantities of the anthocyanin were measured using-Anthocyanin ($\mu g/mL$) = A_{530}–0.24 A_{653}, which is expressed as $\mu g/g$ FW.

Extraction of non-enzymatic antioxidant: Erlenmeyer flask containing 5 g of powder (tissue dried for 72 h in an oven at 60°C) was made with 100 mL of boiling H_2O. After 15 min, the filtrates were collected and adjusted to 100mL with distilled H_2O (Zayneb *et al*., 2015).

Measurement of total flavonoid content: To use the aluminum chloride method (Zhishen *et al*., 1999). 1 mL of the extract with 4 mL of water and 0.3 mL of $NaNO_2$ (5%). 0.3 mL of 10% $AlCl_3$ and 2 mL of sodium hydroxide (1M) were added after 5 min. Once the final water volume was 10mL, the solution was combined. Quercetin was used as the standard. The absorbance was calculated at 510 nm. The amount of quercetin equivalents (QE)-g^{-1} FW used to measure the total content of flavonoid.

Measurement of total phenolic content: To use Folin-Ciocalteu technique (Gulcin, 2020). 200 µL of the extract, 0.8 mL of sodium carbonate (7.5%), and 1 mL of 10% Folin-Ciocalteu were added. The absorbance at 765 nm was determined after 30 min. The reference was gallic acid. Plants were measured for total phenol content (µg) using gallic acid equivalents (GAE)g^{-1} FW.

Total soluble protein content measurement: It was calculated using BSA as a standard with the BioRad reagent. The total amount of soluble protein was represented in mg/FW (Bradford, 1976).

Analyzing the antioxidant enzymes activities: Plant tissues were homogenized (w/v = 1/3; pH 7.5) that contained saccharose (0.4 $mol.L^{-1}$), EDTA-Na_2 (5 $mmol.L^{-1}$), and Tris-HCl (50 $mmol.L^{-1}$). The homogenate was centrifuged at 800 g for 5 min. The supernatant was next centrifuged at 1500 g for 10 minutes. In the homogenization medium, which was kept at 4°C, chloroplast pellets were suspended.

Superoxide dismutase activity (SOD): SOD activity was measured by quantifying the amount of nitroblue tetrazolium photoreduction prevention (NBT) (Kumar *et al*., 2012). Crude extract 100 µL, 50 mM sodium carbonate, 50mM sodium phosphate buffer (pH 7.6), 12 mM L-methionine,0.1 mM EDTA, 50 mM NBT, and 10µM riboflavin were added to make a final volume of 3.0 mL. It was exposed to white light at room temperature for 15 min to activate the SOD. After 15 min incubation, measurement was done at 560 nm. One SOD unit (U) reduced NBT photochemical degradation by 50%.

Catalase (CAT): To measure the catalase activity, the Nandi *et al*., (2019) approach was used. Spectrophotometrically, the CAT activity was determined by observing the decrease in absorbance at 240 nm caused by the room-temperature dissolution of H_2O_2. Unit (U) of catalase activity was defined as the amount of enzyme responsible for a 0.001 change in absorbance per minute during the measurement. The reaction mixture consisted of 30 mM H_2O_2, 100 mM sodium phosphate buffer (pH 7.0), and 100 µL of crude extract in its final volume of 3.0 mL.

Lipid peroxidation estimation: Lipid peroxidation levels were measured using malondialdehyde (MDA) concentrations (Hernández and Almansa, 2002). 1 mL of 0.1% TCA was used to homogenize 100 mg of plant sample. For 10 min at 4°C, the mixture was centrifuged at 15,000 g. 1.5 mL of 0.5% TBA prepared in TCA (20%) was combined with 0.5 mL of supernatant. The mixture was thereafter incubated for 20 min at 90°C. After the reaction was completed, the samples were centrifuged at 10,000 g for 5 min in an ice bath. By subtracting the non-specific absorbance at 600 nm, the absorbance of the supernatant was determined to be 532 nm. An extinction value of 155 mM^{-1} cm^{-1} was used to calculate the amount of MDA that was present.

Statistical analysis

Using one-way analysis of variance (ANOVA), the experimental findings were analyzed, and differences were regarded as significant after they reached the 0.05 threshold of probability. Significant variations between the treatment means are shown in a graph with various letters.

Results

Characterization of CaO NPs

UV-Visible spectroscopy: UV-Visible spectroscopy was used to determine their optical properties, and surface plasmon resonance by measuring light absorption in the UV-Vis range. UV-visible spectra in the current study with wavelengths ranged from 200 to 500 nm (Fig. 2). Broad peaks have been seen at 283 nm, suggesting the presence of CaO NPs.

X-ray diffraction (XRD): Figure 3 displays the XRD patterns of the CaO NPs. The detected XRD peaks and the standard JCPDS file (99-0070), verified a hexagonal structure at all peaks. There were intense peaks at 2θ=32.26, 37.02, 42.33, 53.86, 64.20 and 67.48. Debye Scherer formula (D=Kλ/(βCosθ) was applied to measure the average particle size. The crystallite size of the CaO NPs was then determined to be 24 nm.

Fourier transform infrared spectroscopy (FTIR): The FTIR spectra of CaO NPs are shown in (Fig. 4). Broad peaks at 3433 cm^{-1}, 2808 cm^{-1}, 1422 cm^{-1}, 1166 cm^{-1}, 822 cm^{-1}, and 571 cm^{-1} were obtained. The prominent peak at 3433 cm^{-1} is ascribed to the O-H free hydroxyl bond from the residual hydroxide. The small peaks in the spectra at 2808 cm^{-1} are caused by C-H stretching. Further evidence for the existence of residual hydroxyl groups comes from the presence of absorbance bands in the region ~1600 cm^{-1} and ~800 cm^{-1}. The carbonation of CaO NPs results in the formation of the C-O bond, as seen by the strong broadband at 1422 cm^{-1}, 1166 cm^{-1}, and a peak at 822 cm^{-1}. The Ca–O bond stretch has been shown to have its distinctive peak at 571 cm^{-1}.

Scanning electron microscopy (SEM): SEM provides high-resolution imaging of CaO NPs, revealing their surface morphology. (Fig. 5) represents the SEM image of CaO NPs. The SEM data made clear the high-resolution hexagonal form and the existence of nanoparticle aggregations.

Energy dispersive X-ray spectroscopy (EDX): EDX spectrum (Fig. 6 and Table 1) revealed the elemental composition of CaO NPs. The atomic ratio of calcium and oxygen was observed to be 27.86:72.14, It deviated from the CaO stoichiometry and has a slightly higher oxygen concentration.

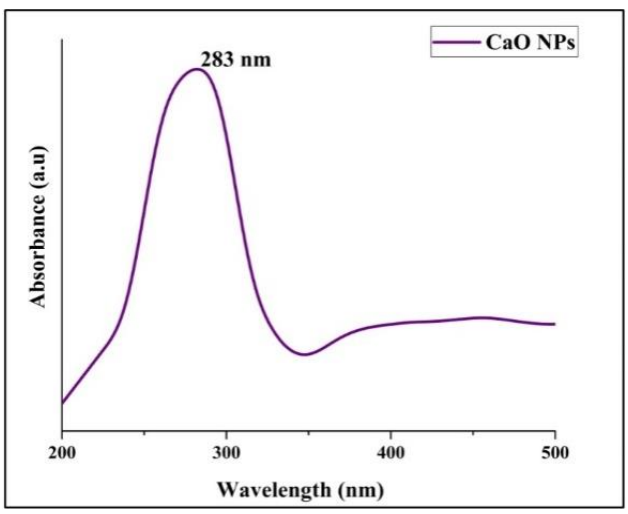

Fig. 2. UV-Visible spectroscopy of CaO NPs.

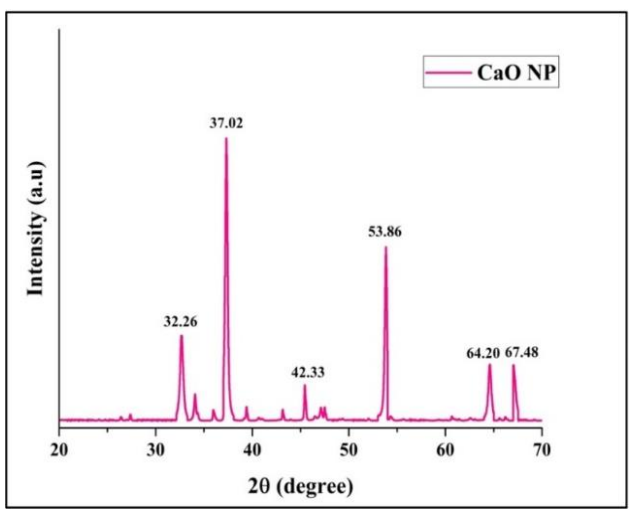

Fig. 3. X-ray Diffraction of CaO NPs.

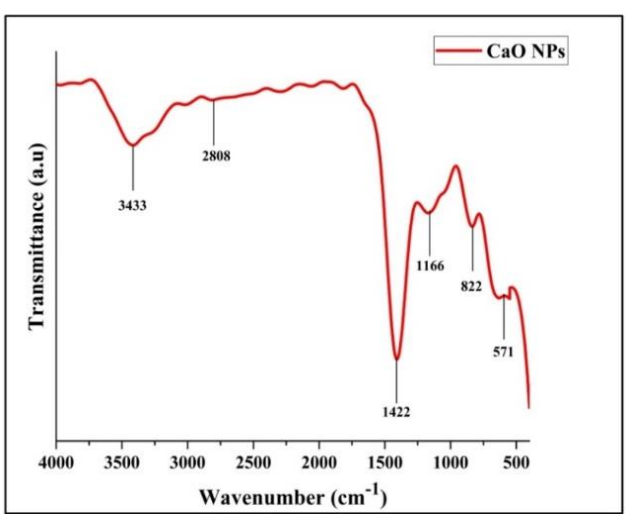

Fig. 4. Fourier transforms the infrared spectrum of CaO NPs.

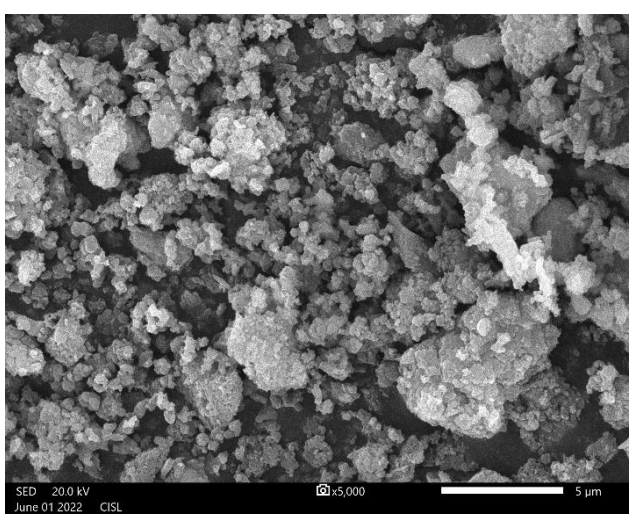

Fig. 5. Scanning electron microscopy image of CaO NPs.

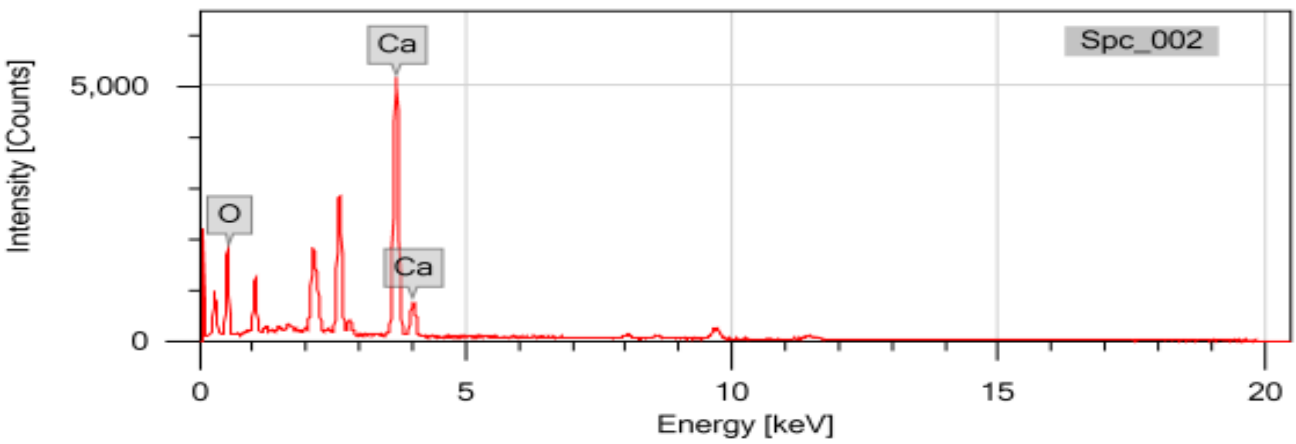

Fig. 6. Energy-dispersive X-ray spectra of CaO NPs.

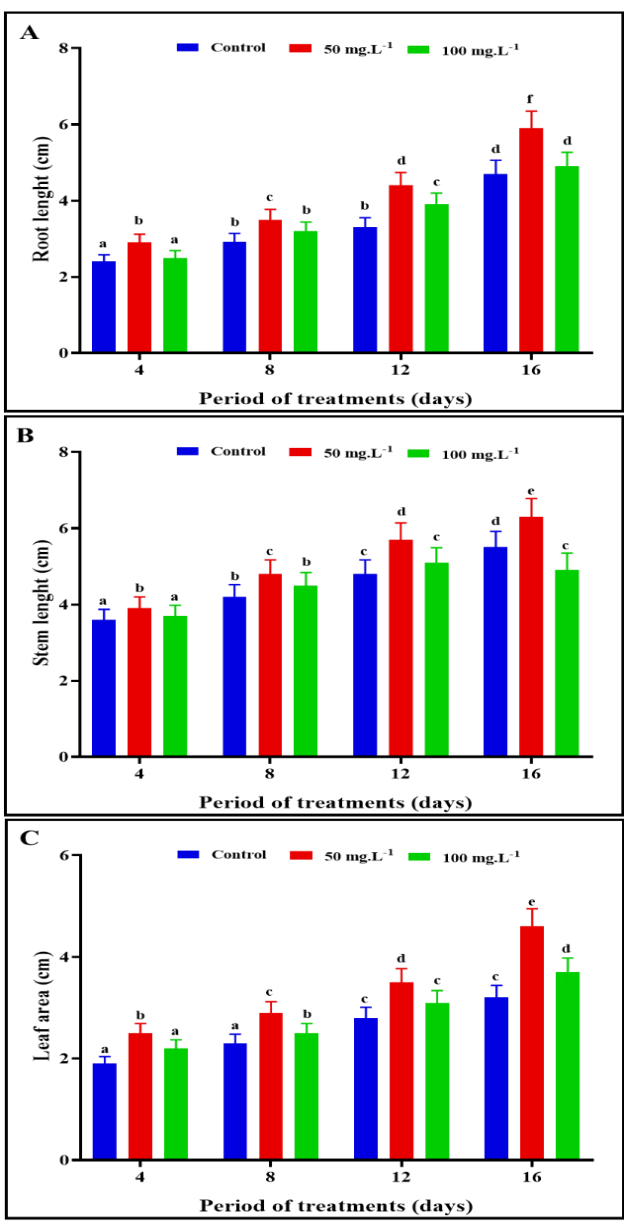

Fig. 7. The effects of CaO NPs treatment at different concentrations (50 and 100 mg/L) on *Trigonella foenum graecum* L., root length (A), stem length (B), and leaf area (C) compared to control. The values represent the mean ± SEM. Alphabets denote the significant variances between the groups (p< 0.05).

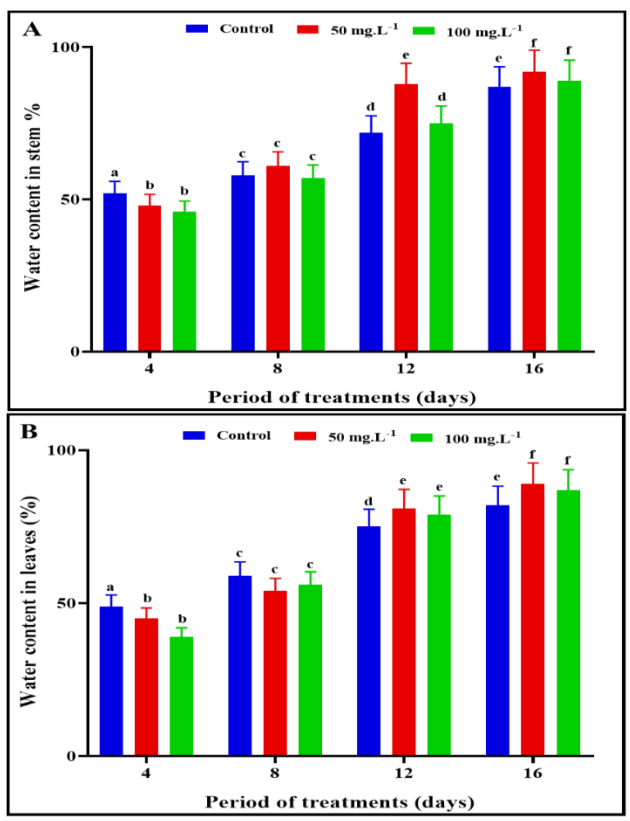

Fig. 8. The effects of CaO NPs treatment at different concentrations (50 and 100 mg/L) on the water content in *Trigonella foenum graecum* L., stem (A) and leaves (B) compared to control. The values represent the mean ± SEM. Alphabets denote the significant variances between the groups (p<0.05).

Effect of CaO NPs on length of stem, root, and leaves area: Figure 7, shows the variation in *Trigonella foenum-graecum* L., root and stem lengths and leaf area. CaO NPs improved root, stem and leaf growth. The root and stem lengths and leaf area were effectively increased on treatment with low concentration (50 mg. L^{-1}) of CaO NPs for 16 days of exposure compared to control. However, the high concentration (100 mg. L^{-1}) of CaO NPs significantly increased the root, stem and leaf growth compared to control, but not that much as in low concentration.

Effect of CaO NPs on water uptake: Figure 8, shows the effect of CaO NPs water content of stem and leaves of

Trigonella foenum-graecum L. When compared to controls, the CaO NPs treated fenugreek stem and leaves had slightly higher water content after 16 days. Moreover, low concentration of CaO NPs had more pronounced effect compared to high concentration.

Effect of CaO NPs on photosynthetic pigment: Figure. 9, shows the effect of CaO NPs on photosynthetic pigment such as chl A, chl B and carotenoids levels in *Trigonella foenum-graecum* L. Photosynthetic pigment contents were increased after 16 days of treatment with 50 mg. L^{-1} of CaO NPs compared to control. As compared to the control and low concentration of CaO NPs, 100 mg. L^{-1} treated groups showed reduced chl A, chl B and carotenoids levels in their leaves.

Effect of CaO NPs on anthocyanin content: Figure 10 shows the effect of CaO NPs on anthocyanin content in *Trigonella foenum-graecum* L. The groups exposed to CaO NPs with 50 mg. L^{-1} concentration had a higher anthocyanin concentration than the controls. However, when compared to control, the high CaO NP concentration (100 mg. L^{-1}) had no impact on the *Trigonella-foenum graecum* L., anthocyanin content (Fig. 10).

Effect of CaO NPs on total flavonoids and phenolics content: Figure 11, shows the effect of CaO NPs on flavonoids and phenolics content of *Trigonella foenum-graecum* L., stem and leaves. The amount of flavonoids in 50 and 100 mg. L^{-1} concentrations of CaO NPs in the stem and leaves were considerably lower than the control. Following a 16-day treatment, 50 mg. L^{-1} and 100 mg.L^{-1} CaO NPs significantly increased the phenol content in both the stem and leaves when compared to the control. Nevertheless, the phenol content in stem and leaves was high in 50 mg. L^{-1} treated seeds compared to 100 mg. L^{-1}.

Effect of CaO NPs on protein content: Figure 12, shows the effect of CaO NPs on protein content of the *Trigonella foenum graecum* L., stem and leaves. The protein in leaves of *Trigonella foenum-graecum* L., with CaO NPs declined more than in control after being subjected to 50 and 100 mg. L^{-1} CaO NPs. In the stem, the amount of protein content was increased upon exposure to 100 mg. L^{-1} CaO NPs, but there was no effect in the concentration of 50 mg. L^{-1} compared to control.

Effect of CaO NPs on antioxidant enzymes: Figure 13, shows the effect of CaO NPs on antioxidant status in *Trigonella foenum graecum* L., stem and leaves. As a consequence of the 16 days of treatment with 50 mg. L^{-1} of CaO NPs in leaves, SOD activity was more significantly increased than controls. In leaves, the SOD activity was slightly reduced on treatment with 100 mg. L^{-1} of CaO NPs for 16 days compared to control. The groups exposed with 50 and 100 mg. L^{-1} of CaO NPs, leaves CAT activity was higher than the control leaves after 16 days of treatment.

In stems, the activity of SOD and CAT was increased on treatment with 50 mg. L^{-1} of CaO NPs after 16 days compared to control groups. On treatment with 100 mg. L^{-1} concentration of CaO NPs, the activity of SOD was slightly increased, but CAT activity was decreased than the control.

Effect of CaO NPs on lipid peroxidation: Figure 14, shows the effect of CaO NPs on lipid peroxidation levels in *Trigonella foenum graecum* L., stem and leaves. MDA content was used to measure lipid peroxidation in the stems and leaves. MDA levels in the leaves treated with 50 mg. L^{-1} and 100 mg. L^{-1} of CaO NPs, were considerably reduced than controls after 16 days of treatment. In stems, after 16 days of exposure to 50 mg. L^{-1} concentration of CaO NPs, MDA levels in CaO NPs treated stems was considerably decreased than controls. But 100 mg. L^{-1} CaO NPs had no effect.

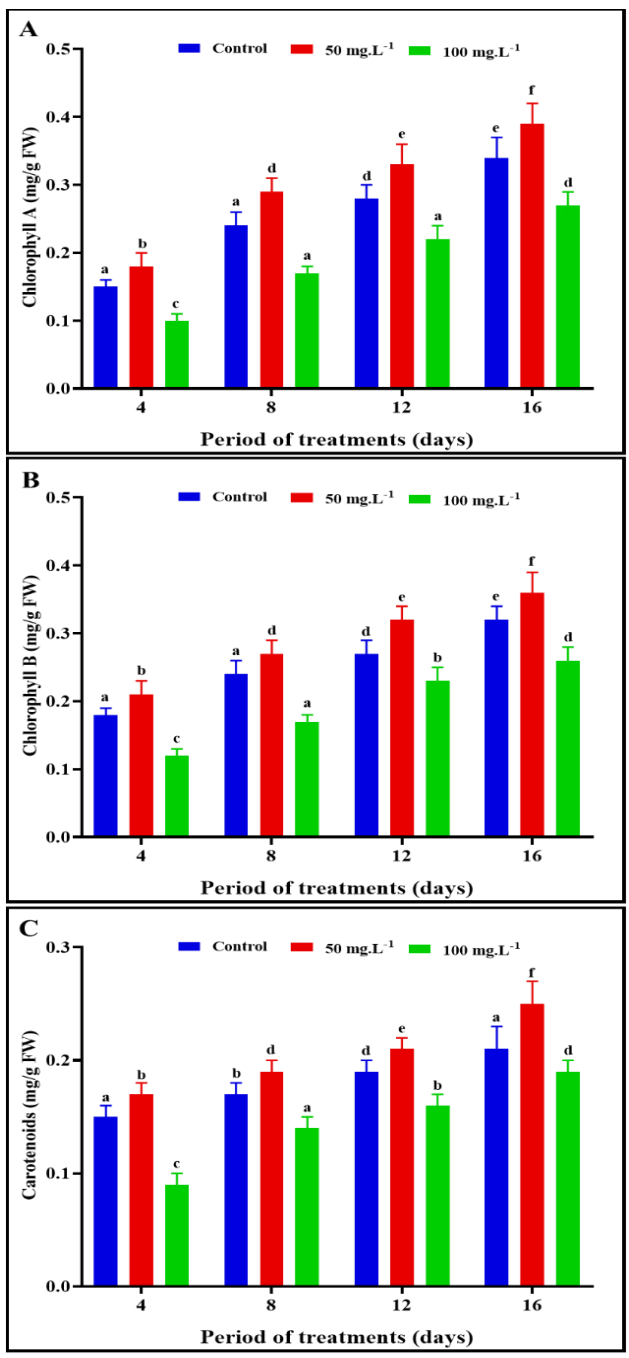

Fig. 9. The effects of CaO NPs treatment at different concentrations (50 and 100 mg/L) on photosynthetic pigments [Chl A (A), Chl B (B) & Carotenoids (C)] content in leaves of *Trigonella foenum graecum* L., compared to control. The values represent the mean ± SEM. Alphabets denote the significant variances between the groups ($p< 0.05$).

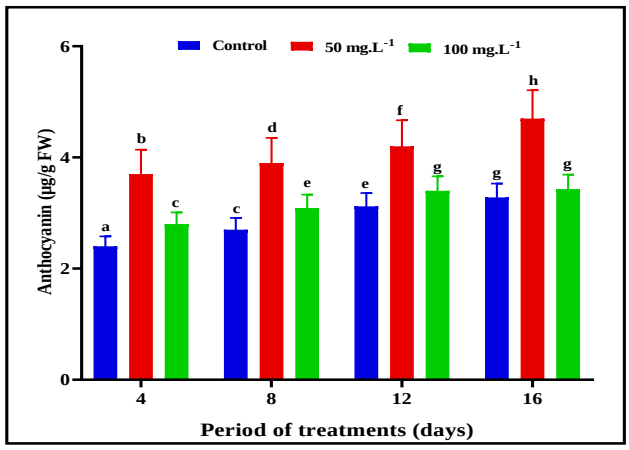

Fig. 10. The effects of CaO NPs treatment at different concentrations (50 and 100 mg/L) on anthocyanin content in *Trigonella foenum graecum* L., compared to control. The values represent the mean ± SEM. Alphabets denote the significant variances between the groups (p<0.05).

Discussion

The application of nanoparticles in agriculture has gained significant interest in recent years due to their potential to enhance crop growth, yield, and stress resistance. In this study, the effects of CaO NPs on the growth and development of *Trigonella foenum-graecum* L., seedlings were investigated at two different concentrations (50 mg. L^{-1} and 100 mg. L^{-1}) over a period of 16 days. The findings revealed a concentration-dependent impact of CaO NPs on various physiological, biochemical, and growth parameters of *Trigonella foenum-graecum* L., seedlings. Figure 15, illustrates the overall research work of CaO NPs on plant growth and development.

In the current investigation, CaO NPs were synthesized by the co-precipitation method. The synthesized CaO NPs have been confirmed by various systemic techniques like UV–visible spectroscopy, XRD, FTIR, SEM, and EDS. We have UV-visible spectra in the ranges of wavelength at 200-500nm. The broad peaks were observed at 283 nm, suggesting the presence of CaO NPs. We detected XRD peaks and the standard JCPDS file (99-0070) verified a hexagonal structure at all peaks. The average size of the particles is 24 nm. The FTIR spectra of CaO NPs show that the Ca–O bond stretch has a distinctive peak at 571 cm^{-1}. The SEM micrograph illustrates the high-resolution hexagonal form and the existence of nanoparticle aggregations. EDX spectrum reveals the appearance of the elements Ca and O in the sample. The atomic ratio of calcium and oxygen was discovered to be 27.86:72.14, It deviates from the CaO stoichiometry and has a slightly higher oxygen concentration.

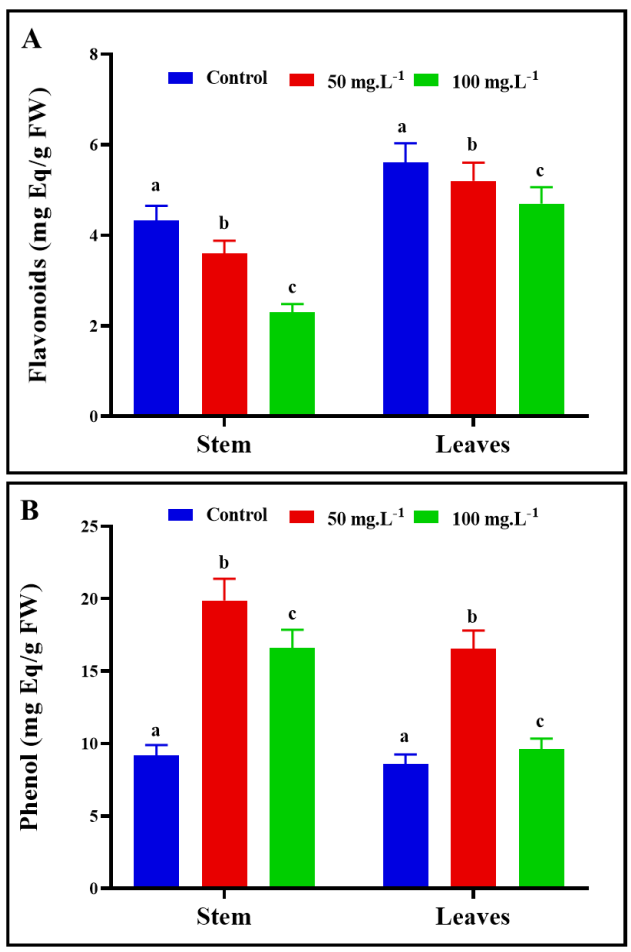

Fig. 11. The effects of CaO NPs treatment at different concentrations (50 and 100 mg/L) on *Trigonella foenum graecum* L., flavonoids (A) and phenols (B) the content in stem and leaves compared to control. The values represent the mean ± SEM. Alphabets denote the significant variances between the groups (p<0.05).

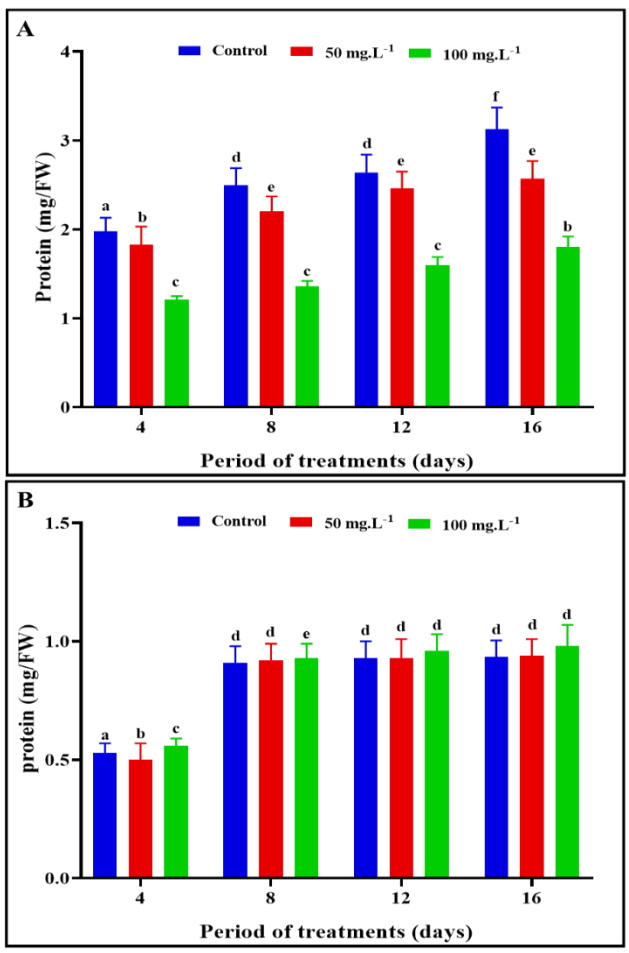

Fig. 12. The effects of CaO NPs treatment at different concentrations (50 and 100 mg/L) on soluble protein content in leaves (A) and stem (B) of *Trigonella foenum graecum* L., compared to control. The values represent the mean ± SEM. Alphabets denote the significant variances between the groups (p<0.05).

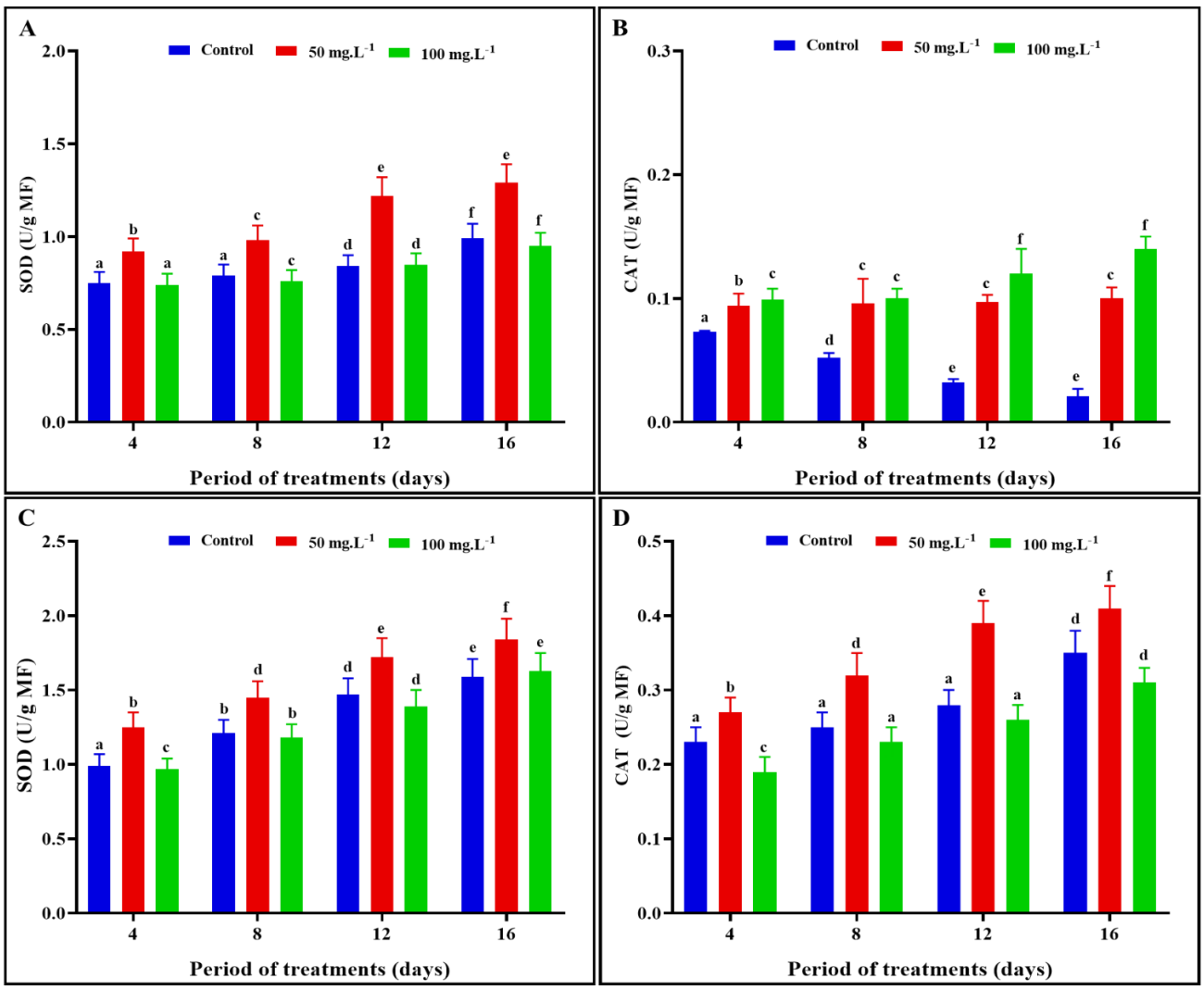

Fig. 13. The effects of CaO NPs treatment at different concentrations (50 and 100 mg/L) on antioxidant enzymes [leaf SOD (A), leaf CAT (B), stem SOD (C) and stem CAT (D)] activities in leaves and stem of *Trigonella foenum graecum* L., compared to control. The values represent the mean ± SEM. Alphabets denote the significant variances between the groups (p<0.05).

The study found that the 50 mg. L^{-1} concentration of CaO NPs had a significant positive impact on the growth of *Trigonella-foenum graecum* L., seedlings, particularly in terms of stem, root, and leaf development. This enhancement in growth can be attributed to the optimal concentration of CaO NPs that may facilitate nutrient uptake, water absorption, and overall metabolic activities in plants. Nanoparticles can penetrate plant tissues more effectively than bulk particles due to their smaller size and larger surface area, which may enhance the availability of nutrients at the cellular level (Wang *et al*., 2023). The increased water content observed in the stems and leaves at both concentrations of CaO NPs, compared to the control, supports this notion. The findings align with Seeger *et al*., (2009), who reported that TiO_2 NPs could enhance transpiration and water use efficiency in willow trees. The increased water content suggests that CaO NPs might have improved the water retention capacity of the cells, potentially leading to better turgor pressure and cell expansion.

However, at a higher concentration of 100 mg. L^{-1}, the impact on growth parameters was less pronounced, and in some cases, it even resulted in a decline compared to the control. This suggests a threshold beyond which the beneficial effects of CaO NPs diminish, and potentially harmful effects begin to manifest. High concentrations of NPs can cause toxicity, oxidative stress, and cell membrane damage, leading to reduced growth and development in plants.

Photosynthetic pigments, including chl A, chl B, and carotenoids, play a crucial role in capturing light energy for photosynthesis, and their levels are often indicators of the overall health and productivity of plants. In this study, the highest levels of chl A, chl B, and carotenoids were observed at 50 mg. L^{-1} CaO NP exposure, whereas a decrease in these pigments was noted at 100 mg. L^{-1}. This trend is consistent with the findings of Usman *et al*., (2020), who reported that low concentrations of Ag NPs increased chlorophyll content in maize plants, while higher concentrations reduced it.

The increase in photosynthetic pigments at 50 mg. L^{-1} suggests that CaO NPs at this concentration could enhance the light-harvesting capacity of *Trigonella foenum-graecum* L., seedlings, potentially leading to improved

photosynthetic efficiency and growth. Conversely, the decrease in pigment levels at 100 mg. L^{-1} indicates that higher concentrations may cause stress or toxicity, which could impair chloroplast function and reduce the synthesis of chlorophyll and carotenoids. Such effects may be associated with the generation of reactive oxygen species (ROS) and oxidative damage to chloroplast membranes, as observed in other studies involving different types of nanoparticles (Lei *et al*., 2008).

Table 1. EDX Analysis of CaO NPs.

Element	Mass%	Atom%
O	50.83 ± 0.54	72.14 ± 0.77
Ca	49.17 ± 0.28	27.86 ± 0.16

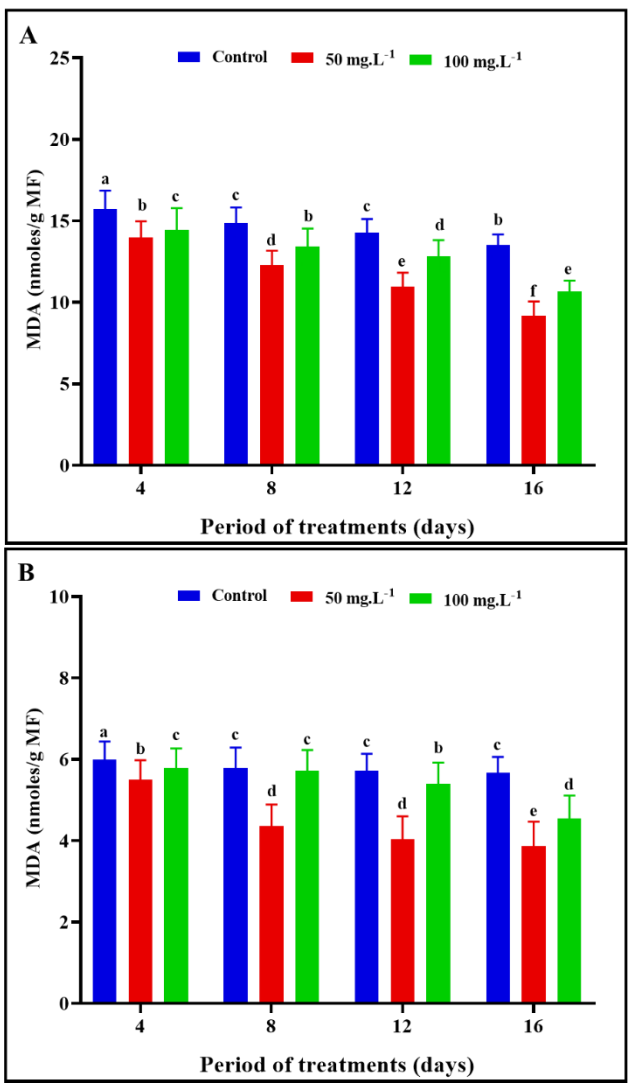

Fig. 14. The effects of CaO NPs treatment at different concentrations (50 and 100 mg/L) on MDA concentration in *Trigonella foenum graecum* L., seedlings leaves (A) and stems (B) compared to control. The values represent the mean ± SEM. Alphabets denote the significant variances between the groups (p<0.05).

Anthocyanins and flavonoids are important secondary metabolites that play key roles in plant defense against abiotic and biotic stress, as well as in attracting pollinators and seed dispersers. The study found that the application of 50 mg. L^{-1} CaO NPs significantly increased anthocyanin content in *Trigonella foenum-graecum* L., seedlings compared to the control, while 100 mg. L^{-1} had no significant effect. This pattern was similar to the findings of Kumar *et al*., (2012), who reported that low concentrations of Pb increased anthocyanin content in Ceylon spinach.

The increased anthocyanin content at 50 mg. L^{-1} CaO NPs may be attributed to the activation of the phenylpropanoid pathway, which is catalyzed by phenylalanine ammonium-lyase (PAL). However, at higher concentrations of 100 mg. L^{-1}, the generation of excessive ROS, such as H_2O_2, may inhibit PAL activity, thereby reducing anthocyanin synthesis (Kitamura *et al*., 2002). This suggests a concentration-dependent effect where optimal concentrations stimulate anthocyanin production, while higher concentrations lead to oxidative stress that hampers metabolic pathways involved in secondary metabolite production.

Flavonoid levels were found to decrease at both concentrations of CaO NPs compared to the control, indicating that the treatment may not favor flavonoid biosynthesis in *Trigonella foenum-graecum* L., seedlings. This could be due to the differential regulation of secondary metabolite pathways in response to nanoparticle exposure. In stem and leaves, phenol levels were increased at both concentrations compared to control. However, it significantly increased at 50 mg. L^{-1} CaO NPs treatment.

Protein levels are critical indicators of the metabolic status and overall health of plants. The study showed that protein levels decreased at both concentrations of CaO NPs in leaves, while in stems, 50 mg. L^{-1} CaO NPs had no effect, and 100 mg. L^{-1} showed limited impact. These results are consistent with the findings of Ali *et al*., (2021), who demonstrated that the effects of AgNPs on common beans and maize were concentration-dependent, with low concentrations enhancing protein content and higher concentrations leading to a decline. The decrease in protein content observed at both concentrations in leaves could be associated with nanoparticle-induced stress, which affects protein synthesis or leads to protein degradation. The direct correlation between chlorophyll content and protein levels (Ren *et al*., 2011) further supports this, as reduced chlorophyll levels at higher NP concentrations would likely correspond to lower protein synthesis.

Antioxidant enzymes such as SOD and CAT are essential components of the plant defense system against oxidative stress. The results showed a significant increase in SOD and CAT activities at 50 mg. L^{-1} CaO NPs in both leaves and stems, whereas no such enhancement was observed at 100 mg.L^{-1}. This suggests that a moderate concentration of CaO NPs can activate the plant's antioxidant defense system, thereby protecting it from oxidative damage. These findings were in agreement with Zia *et al*., (2021), who reported increased CAT activity at low to moderate concentrations of TiO_2 NPs but reduced activity at higher concentrations in onion seed germination. The enhanced activities of SOD and CAT at 50 mg. L^{-1} may help in scavenging ROS and maintaining cellular redox homeostasis, which is crucial for growth and development. At 100 mg. L^{-1}, the antioxidant defense may be overwhelmed by excessive ROS production, leading to oxidative stress and cellular damage.

MDA is a widely used marker for lipid peroxidation and membrane damage under stress conditions. The study revealed that MDA concentrations in leaves treated with both 50 and 100 mg. L^{-1} of CaO NPs were significantly lower than in the control, suggesting reduced lipid peroxidation and better membrane stability. In stems, MDA levels were significantly decreased at 50 mg. L^{-1} but showed no significant change at 100 mg. L^{-1} compared to the control. The decrease in MDA levels at 50 mg. L^{-1} indicates that this concentration of CaO NPs may protect cellular membranes from oxidative damage, possibly by enhancing antioxidant enzyme activities and reducing ROS accumulation. This protective effect is in line with previous research, which shows that moderate NP concentrations can enhance stress tolerance in plants (Lei *et al*., 2008). However, the lack of effect at 100 mg. L^{-1} suggests that higher concentrations may not provide additional benefits and could potentially lead to adverse effects.

The experiment demonstrated that while CaO NPs effectively enhanced *Trigonella foenum-graecum* L., growth at lower concentrations (50 mg. L^{-1}), whereas higher concentrations (100 mg. L^{-1}) led to stagnation or minimal impact on growth, revealing a concentration-dependent response. Positive outcomes at low concentrations included increased root and stem length, larger leaf area, and improved biochemical markers like chlorophyll content and antioxidant activity. Future research should explore optimizing concentrations to maximize benefits while minimizing adverse effects.

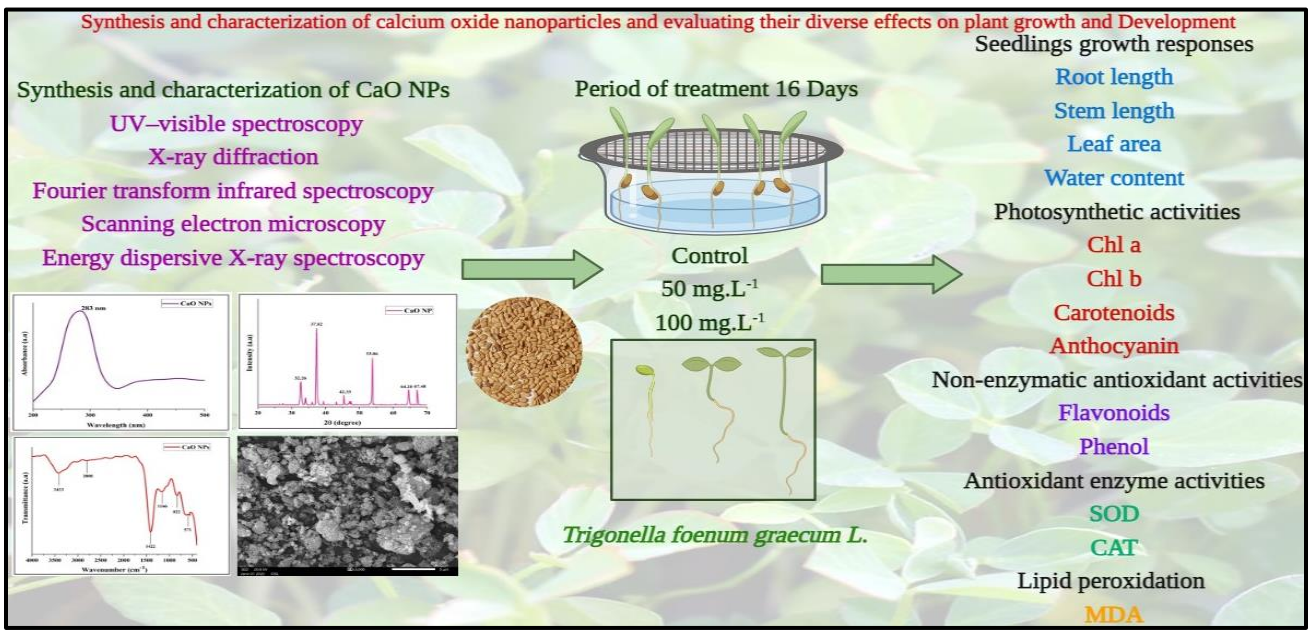

Fig. 15. Schematic illustration of diverse effects of CaO NPs on plant growth and development of *Trigonella foenum graecum* L.

Conclusion

In conclusion, this study demonstrates that CaO NPs have a concentration-dependent impact on *Trigonella foenum-graecum* L., seedlings. While 50 mg. L^{-1} CaO NPs promote growth and enhance physiological parameters, a higher concentration of 100 mg. L^{-1} may lead to toxicity and oxidative stress, resulting in neutral or adverse effects. These findings align with previous research on other NPs, emphasizing the need to optimize NP concentrations for agricultural purposes. Future studies should explore the molecular mechanisms of NP uptake and effects, as well as conduct long-term assessments in diverse plant species under field conditions to ensure the safe and effective use of NPs in agriculture.

Acknowledgement

The authors are grateful to the Department of Biochemistry and Biotechnology at Annamalai University, Chidambaram for their assistance in supplying lab space along with all other required equipment and materials.

Funding: This article is derived from a research grant funded by the Research, Development, and Innovation Authority (RDIA) - Kingdom of Saudi Arabia with grant number (13445-Tabuk-2023-UT-R-3-1-SE).

References

Ali, S.S., R. Al-Tohamy, E. Koutra, M.S. Moawad, M. Kornaros, A.M. Mustafa, Y.A.G. Mahmoud, A. Badr, M.E. Osman T. Elsamahy and H. Jiao. 2021. Nanobiotechnological advancements in agriculture and food industry: Applications, nanotoxicity, and future perspectives. *Sci. Total Environm.*, 792, p.148359.

Amin Alavi, M. and A. Morsali. 2010. Ultrasonic-assisted synthesis of Ca (OH) 2 and CaO nanostructures. *J. Experim. Nanosci.*, 5(2): 93-105.

Bharathiraja, B., M. Sutha, K. Sowndarya, M. Chandran, D. Yuvaraj and R. Praveen Kumar. 2018. Calcium oxide nanoparticles as an effective filtration aid for purification of vehicle gas exhaust. *Adv. Internal Combust. Engine. Res.*, 181-192.

Bradford, M.M. 1976. A rapid and sensitive method for the quantitation of microgram quantities of protein utilizing the principle of protein-dye binding. *Analytical Biochem.*, 72(1-2): 248-254.

Cakmak, I. and H. Marschner. 1992. Magnesium deficiency and high light intensity enhance activities of superoxide dismutase, ascorbate peroxidase, and glutathione reductase in bean leaves. *Plant Physiol.*, 98(4): 1222-1227.

El-Briak, H., D. Durand, J. Nurit, S. Munier, B. Pauvert and P. Boudeville. 2002. Study of a hydraulic dicalcium phosphate dihydrate/calcium oxide-based cement for dental applications. *J. Biomed. Mater. Res: An Official Journal of The Society for Biomaterials, The Japanese Society for Biomaterials, and The Australian Society for Biomaterials and the Korean Society for Biomaterials*, 63(4): 447-453.

Gamborg, O.L. and L.R. Wetter. 1975. Plant tissue culture methods. Saskatoon: National research council of Canada. Prairie regional laboratory, 1975.

Gould, K.S., K.R. Markham, R.H. Smith and J.J. Goris. 2000. Functional role of anthocyanins in the leaves of Quintinia serrata A. Cunn. *J. Experim. Bot.*, 1107-1115.

Gulcin, İ. 2020. Antioxidants and antioxidant methods: An updated overview. *Archives Toxicol.*, 94(3): 651-715.

Habte, L., N. Shiferaw, D. Mulatu, T. Thenepalli, R. Chilakala and J.W. Ahn. 2019. Synthesis of nano-calcium oxide from waste eggshell by sol-gel method. *Sustainability*, 11(11): 3196.

Hernández, J.A. and M.S. Almansa. 2002. Short-term effects of salt stress on antioxidant systems and leaf water relations of pea leaves. *Physiologia Plantarum*, 115(2): 251-257.

Jadhav, V., A. Bhagare, S. Wahab, D. Lokhande, C. Vaidya, A. Dhayagude, M. Khalid, J. Aher, A. Mezni and M. Dutta. 2022. Green synthesized calcium oxide nanoparticles (CaO NPs) using leaves aqueous extract of *Moringa oleifera* and evaluation of their antibacterial activities. *J. Nanomat*, 2022(1): p. 9047507.

Kitamura, Y., M. Ohta, T. Ikenaga and M. Watanabe. 2002. Responses of anthocyanin-producing and non-producing cells of *Glehnia littoralis* to radical generators. *Phytochemistry*, 59(1): 63-68.

Kumar, A., S. Dutt, G. Bagler, P.S. Ahuja and S. Kumar. 2012. Engineering a thermo-stable superoxide dismutase functional at sub-zero to> 50 C, which also tolerates autoclaving. *Scientific Reports*, 2(1): 387.

Kumari, M., B. Sarkar and K. Mukherjee. 2023. Nanoscale calcium oxide and its biomedical applications: A comprehensive review. *Biocatalysis & Agricult. Biotechn.*, 47, p.102506.

Lei, Z., S. Mingyu, W. Xiao, L. Chao, Q. Chunxiang, C. Liang, H. Hao, L. Xiaoqing and H. Fashui. 2008. Antioxidant stress is promoted by nano-anatase in spinach chloroplasts under UV-B radiation. *Biological Trace Element Res.*, 121: 69-79.

Nandi, A., L.J. Yan, C.K. Jana and N. Das. 2019. Role of catalase in oxidative stress-and age-associated degenerative diseases. *Oxidative Medicine and Cellular Longevity*, 2019(1): 9613090

Reid, J.G. 1971. Reserve carbohydrate metabolism in germinating seeds of *Trigonella foenum-graecum* L. (Leguminosae). *Planta*, 100: 131-142.

Ren, H.X., L. Liu, C. Liu, S.Y. He, J. Huang, J.L., Li, Y. Zhang, X.J. Huang and N. Gu. 2011. Physiological investigation of magnetic iron oxide nanoparticles towards Chinese mung bean. *J. Biomedical Nanotechn.*, 7(5): 677-684.

Seeger, E.M., A. Baun, M. Kästner and S. Trapp. 2009. Insignificant acute toxicity of TiO 2 nanoparticles to willow trees. *J. Soils & Sediments*, 9: pp. 46-53.

Srinivasan, M.K., B.J. Premnath, R. Parimelazhagan and N. Namasivayam. 2024. Synthesis, characterization, and evaluation of the anticancer properties of pH-responsive carvacrol-zinc oxide quantum dots on breast cancer cell line (MDA-MB-231). *Cell Biochemistry & Function*, 42(4), p. e4062.

Syed, Q. A., Z. Rashid, M. H. Ahmad, R. Shukat, A. Ishaq, N. Muhammad and H. U. U. Rahman. 2020. Nutritional and therapeutic properties of fenugreek (Trigonella foenum-graecum): a review. *International Journal of Food Properties*, 23(1): 1777-1791.

Tang, Z.X., D. Claveau, R. Corcuff, K. Belkacemi and J. Arul. 2008. Preparation of nano-CaO using thermal-decomposition method. *Materials Letters*, 62(14): 2096-2098.

Usman, M., M. Farooq, A. Wakeel, A. Nawaz, S.A. Cheema, H. ur Rehman, I. Ashraf and M. Sanaullah. 2020. Nanotechnology in agriculture: Current status, challenges and future opportunities. *Science Total Environ.*, 721: 137778.

Venkatesan, K.B., S. Alamelu, S.R. Priya, N. Jayaseelan, S.K. Kamaraj, M.K. Srinivasan, M.A. Alshehri, C. Panneerselvam, A. Saif and S. Periyasamy. 2023. Ameliorated antimicrobial, antioxidant, and anticancer properties by *Plectranthus vettiveroides* root extract-mediated green synthesis of chitosan nanoparticles. *Green Processing & Synthesis*, 12(1): p. 20230086.

Visuvanathan, T., L.T.L. Than, J. Stanslas, S.Y. Chew and S. Vellasamy. 2022. Revisiting *Trigonella foenum-graecum* L.: Pharmacology and Therapeutic Potentialities. *Plants.,* 11(11): 1450.

Wang, X., H. Xie, P. Wang and H. Yin. 2023. Nanoparticles in plants: uptake, transport and physiological activity in leaf and root. *Materials*, 16(8): 3097.

Zayneb, C., K. Bassem, K. Zeineb, C.D. Grubb, D. Noureddine, M. Hafedh and E. Amine. 2015. Physiological responses of fenugreek seedlings and plants treated with cadmium. *Environm. Science & Pollution Res.*, 22: 10679-10689.

Zhishen, J., T. Mengcheng and W. Jianming. 1999. The determination of flavonoid contents in mulberry and their scavenging effects on superoxide radicals. *Food Chem.*, 64(4): 555-559.

Zia, R., M.S. Nawaz, M.J. Siddique, S. Hakim and A. Imran. 2021. Plant survival under drought stress: Implications, adaptive responses, and integrated rhizosphere management strategy for stress mitigation. *Microbiol. Res.*, 242, p. 126626.

(Received for publication 23 February 2024)